Emergent Materials (2022) 5:1409–1427
https://doi.org/10.1007/s42247-021-00261-y

REVIEW

Thin-film composite nanofiltration hollow fiber membranes toward textile industry effluent treatment and environmental remediation applications: review

Ankush D. Sontakke[1] · Pranjal P. Das[1] · Piyal Mondal[1] · Mihir K. Purkait[1]

Received: 2 June 2021 / Accepted: 3 July 2021 / Published online: 16 July 2021

Abstract
Hollow fiber (HF) membranes are considered one of the emerging technologies in the field of membrane separation. It has undergone massive development for its various efficient applications during the past few decades. To further improve and develop the membrane technology, HF membranes have been fabricated for the nanofiltration (NF) process and found to yield higher efficiencies toward various environmental remediation applications. In this work, an elaborate discussion on the various fabrication methods and advantages of thin-film composite (TFC) NF HF membranes in the field of separation processes was listed. Moreover, the surface functionalization of such membranes to provide better separation efficiency is critically reviewed. The utilization of such thin-film HF membranes in several environmental remediation applications such as treating textile industry wastewater and other operations such as heavy metal removal, organic micropollutant removal, and inorganic salt removal has been explored in detail in this chapter. Further to this, the scope of improvements has been discussed in the conclusion section, which may enhance the overall efficiency of the thin-film composite NF HF membrane. This article will be much beneficial to the researchers for acquiring in-depth knowledge on the latitudes of various TFC HF fabrication methods, its functionalization, and wide ranges of promising environmental remediation applications.

Keywords Hollow fiber membrane · Nanofiltration · Nanocomposite · Heavy metal removal · Dye removal

1 Introduction

In today's world, the scarcity of potable water has triggered significant challenges for humans as well as animals and plants. The present shortage of water in the twenty-first century has become a global issue with most countries throughout the world. The rapid infrastructural and industrial development is the primary cause for the paucity of potable water as it produces various forms of water contaminants along with environmental pollutants. For example, in textile industries, it was reported that throughout the world, nearly 7×10^5 tons of dye-related products are produced, and for 1 ton of the product, around 200–350 m^3 of contaminated water is inevitably generated [1, 2]. Also, the comprehensive increase in human population and environmental pollution are particularly accountable aspects for the water crisis. As per WHO, by 2025, nearly half of the world's population will be living in water-stressed areas due to water scarcity [3, 4]. Therefore, it has become essential to manage the freshwater resources and develop novel technologies for wastewater treatment and its reuse to ensure passable water quantity and quality.

Meanwhile, the scarcity of clean water resources demands the development of economical and efficient technologies for decontamination of polluted water along with innovative technologies for seawater desalination. In order to address this global threat of clean water and environmental pollution, various ongoing researches explored new green methodologies, technological innovations, and novel materials for minimizing the water pollutants, recycling of valuable products,

✉ Piyal Mondal
piyal@iitg.ac.in

Ankush D. Sontakke
ankus176107025@iitg.ac.in

Pranjal P. Das
pranj176107027@iitg.ac.in

Mihir K. Purkait
mihir@iitg.ac.in

[1] Department of Chemical Engineering, Indian Institute of Technology, Guwahati, Assam 781039, India

and reusing contaminated water after treatment. The conventional methods for water purification had attracted great attention toward the treatment of wastewater due to easy processing and low expenditures. The method includes electrocoagulation [5, 6], chemical precipitation [7], disinfection by oxidation/ozonation [5], carbon adsorption [8], membrane filtration [9–11], and chemical or biological degradation [12, 13]. The applicability of these methods is based on the pollutant removal efficiency, cost, and overall energy consumption based on separation efficiency rate.

In the past decade, with the consideration of the methods mentioned earlier, membrane separation technology has gained enormous attention due to selective permeation, lower energy consumption, and higher throughput and non-thermal processing [14]. The recent advancement in polymeric and ceramic materials and their composites by the inclusion of novel nanomaterials has made their widespread use in the fabrication of composite membranes. The modified composite membranes showed their applicability toward separating contaminants like heavy materials, anionic, and cationic dyes [15, 16]. Also, the newly developed nanomaterials with enhanced surface properties and separation ability provided innovative approaches for removing water pollutants via their incorporation in membranes. The membrane separation processes are mainly divided into microfiltration (MF), ultrafiltration (UF), nanofiltration (NF), and reverse-osmosis (RO) processes. The NF membrane separation is a pressure-driven process; the nominal pore size of NF membrane and molecular weight cutoff (MWCO) lies between 0.5 and 2 nm and between 200 and 1000 Da, respectively [17]. In NF membrane, the separation mechanism is based on two principles, namely, size exclusion, i.e., steric effect and electrostatic interaction between membrane surface and feed solution, i.e., Donnan exclusion. The NF membranes are capable to retard low molecular weight compounds, heavy metals, nitrates, and sulfates along with colors and tannins. Also, the NF membrane filtration possesses a lower retention concentration with lower discharge volume than RO membranes [18]. Since the last few decades, NF-based membrane separation has become an important process for removing water contaminants from the steel, textile, and pharmaceutical industries. The NF membranes are also utilized for the separation of organic pollutants, organic solvents, and ionic liquids [19].

Along with the separation efficiency and flux, mechanical strength and robustness are the crucial factors of the membrane. The hollow fiber (HF) membrane with higher membrane surface area per unit volume of the membrane module, easy handling, and self-supporting assembly provides several advantages over flat sheet membrane[15, 19, 20]. Recently, the HF membranes with unique characteristics have gained a growing interest for different water treatment-related applications such as heavy metal removal [21], dye removal, and desalination [22, 23]. The HF membrane assembly also provides the membrane modification facility by coating thin active layers of different nanomaterials to improve separation efficiency. The modified thin-film composite (TFC) HF membrane consists of a nano-thin selective and dense layer at the top and a porous substrate at the bottom, which provides the required mechanical support to the membrane. However, by modifying the selective top layer and the porous substrate, the overall performance of the membrane can be enhanced. The top dense layer of the membrane can be modified by several functional materials and inorganic materials such as polyamides (PA), graphene oxide (GO) and GO nanoscrolls, zeolites, TiO_2, and metal-organic frameworks (MOFs) [15, 24, 25]. Recently, Li et al. (2021) fabricated a thin eGO/PA NF membrane over a porous HF ceramic membrane using interfacial polymerization technique for efficient removal of heavy metals. The two-dimensional GO was modified with ethylene diamine (EDA) and expertly impregnated over the surface of the hollow fiber ceramic (HFC) substrate without involving the interlayers. The obtained membrane had successfully removed the heavy metals such as Cu^{2+}, Pb^{2+}, Ni^{2+}, and Zn^{2+} with a removal rate of >88% [26]. Similarly, Ji et al. (2021) developed a green solvent-free process-based PVDF loose NF HF membrane of TFC multilayer structure. The obtained membrane had presented higher negative dyes rejection (>98.5%) and lower salt rejection (~4%) simultaneously for a continuous 360-min run. The membrane had shown excellent potential for textile wastewater treatment [23].

The TFC NF HF membranes have shown a superior separation performance over flat sheet membranes for permeability, flux, removal efficiency, and low energy consumption to that of RO membranes over the past few years. Despite several advantages and great potential of TFC NF HF membrane for wastewater treatment and environmental remediation-related applications, it is envisaged that the studies related to its application in textile industries are very limited. Again, a review of NF HF membrane describing the significance and limitations in state-of-art literature on fabrication methods and modification in a thin selective layer of TFC membrane for removal of heavy metals, dyes from textile industries, organic micropollutants, and inorganic salts is scant. The main objective of this review is to discuss in detail the criticalities related to fabrication, functionalization, and application of TFC NF HF membrane for treatment of textile industrial effluent and other possible applications toward environmental remediation. It is thus proposed that the review study presented here is the first-ever dedicated work over applications of TFC NF HF membrane in environmental remediation. It is believed that the provided information will be helpful to the readers to acquire adequate knowledge on the TFC NF HF membrane and its possible applications.

2 Advantages of hollow fiber membrane for nanofiltration

The industrial, infrastructural, technological, and overall economic developments lead to environmental pollution, which is increasing sparingly while affecting the water bodies and indirectly the human health. The experts, as well as the public, are very much concerned about water contamination. The requirement of clean water urges several technological advancements like membrane filtration processes such as nanofiltration. As discussed before, NF is a pressure-driven membrane separation process with the characteristics that lie between UF and RO [17]. The NF membranes are capable of the removal of dissolved solids along with a selective rejection of multivalent and limited monovalent ions with better permeability and less energy requirements than RO. NF membranes can be fabricated and module in various geometries like a flat sheet, tubular, or cylinder [20].

Presently, NF membranes are widely used for the treatment of domestic and industrial wastewater. The NF HF geometry provides several advantages over spiral-wound module flat sheet membranes and tubular membranes. The spiral-wounded modules possess higher head losses within spacer channels during the filtration process, which results in higher energy requirements; also, they do not provide a backflushing facility, which results in fouling due to suspended solids over the surface and spacers. However, the tubular membranes are less vulnerable to fouling and require a facile cleaning approach but have a lower packing density of 400–800 m^2/m^3, nearly identical to spiral-wound membranes (300–1000 m^2/m^3) [20, 27]. In contrast to tubular membranes and flat sheet spiral-wound membranes, the HF membranes have a higher packing density of 300–1700 m^2/m^3 and require less maintenance with the pretreatments process [20]. The significant characteristics of HF membrane include a higher surface-to-volume ratio, packing density and permeability with self-supportive assembly, lower energy requirement, and ease in handling. The basic morphologies of HF membranes are isotropic or anisotropic, porous or dense, and composite types. Such distinctive characteristics of HF membranes provide them outstanding properties for mass transfer operations, which promotes several real-life applications in various fields like water treatment (desalination and decontamination) and pharmaceutical industries (separation and purification) [4]. Moreover, the HF membranes due to its outstanding features have been successfully explored for the mass transfer operations such as gas and liquid separation by membrane contactors [28], dialysis in the medical field [29], pervaporation for separation of azeotropic mixtures[30], desalination via membrane distillation [31, 32] and separations and concentrating operation in food industries [4].

The HF membrane substrates can be fabricated using polymers like poly(vinylidene fluoride) (PVDF), poly(acrylonitrile) (PAN), poly(amide) (PA), poly(ether sulfone) (PES), cellulose acetate (CA), and ceramic materials [15, 26] using melt spinning, dry spinning, dry-jet wet spinning, and wet spinning. However, the TFC HF membranes are fabricated employing Interfacial polymerization, phase inversion, dip coating, plasma treatment, and chemical reaction [15]; the details are provided in a subsequent section. The fabricated HF membranes are mainly assembled in-cylinder module and HF flat-plate membrane module, as shown in Fig. 1. The assembly comprises a number of HF membranes, which provides higher productivity via a larger surface area and packing density [4].

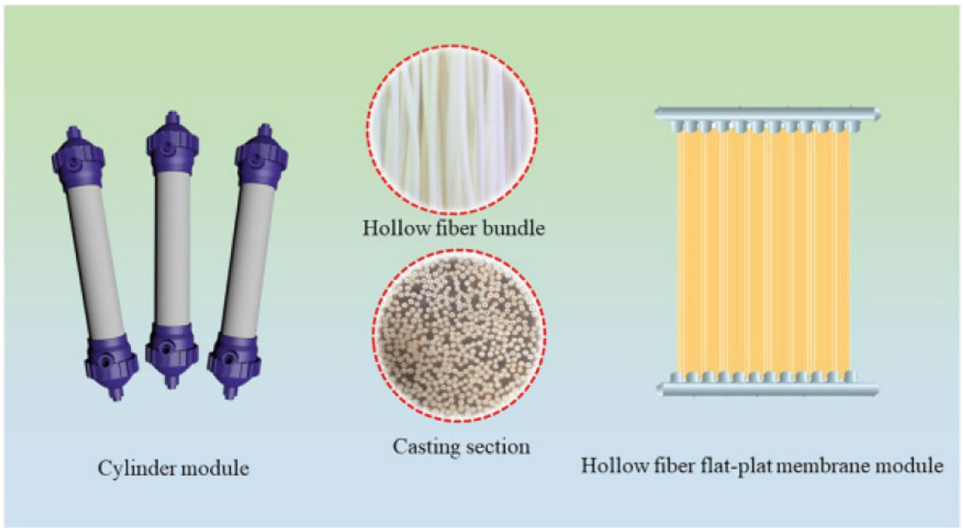

Fig. 1 Hollow fiber membrane modules. Reproduced with permission [4]

3 Fabrication methods for TFC NF hollow fiber membrane

The supreme membranes should have better permeability, stable flux, better mechanical strength with good chemical stability, and durability. Generally, the chemical composition of membrane material decides the chemical and thermal stability of the membrane. Over the decades, several studies related to fabrication, characterization, and application of the HF membranes have been reported with different polymeric materials. Once the material is selected, the permeability and mechanical strength of the membrane can be determined by the structure of the membrane [4, 15, 20]. However, membrane structure depends on the process and technique utilized for membrane fabrication. In membranes, the selectivity and permeability, along with the mechanical strength, particularly the resistance in chemical cleaning process and robustness, are also important factors. Presently, a great majority of commercial membranes are fabricated via the non-solvent induced phase separation (NIPS) technique. These HF membranes are self-supportive and can be damaged in real-time applications due to the impact of water flow, long-time high pressure, and frequent cleaning [4]. Therefore, it is obligatory to fabricate the HF membranes with better mechanical strength and separation characteristics, and it solely depends on the membrane materials and fabrication techniques. By considering the importance of fabrication methods, herein, an attempt has been made to explore the basic fabrication methods along with the recent advancements in HF membrane substrates and TFC. Also, the methods available for the fabrication of HF membrane and TFC HF membranes are critically reviewed and discussed in the subsequent section.

3.1 Fabrication of pristine hollow fiber substrates

The HF membrane can be homogeneous or asymmetric, dense, or porous and of a composite type. Different fabrication approaches are adapted for the production of HF membranes, including melt spinning and solution spinning. The melt spinning process is mainly used to fabricate dense and homogenous HF membranes, while the solution spinning process is adapted for porous and asymmetric membrane fabrication. The solution spinning method is again subdivided into three different processes: dry spinning, dry-jet wet spinning, and wet spinning [14, 15, 33]. However, the asymmetric HF membranes are mostly fabricated via a dry-jet wet spinning method. The details related to fabrication methods and factors affecting the membrane characteristics and spinning process are briefed as below.

3.1.1 Melt spinning

In this process, the primary mechanism behind the HF membrane formation is the phase transformation of solid thermoplastic polymer into melted liquid. The properties of membranes obtained by melt spinning are primarily dependent on the rheology and cooling rate of the polymer melt. Herein the extruder is used for melting and transporting polymer melt to melt pump, which then flows through the die, i.e., spinneret and cooled in air subsequently to form an HF membrane.

3.1.2 Dry spinning

In the dry spinning process, initially, the polymer is dissolved in the appropriate solvent such as NMP, DMF, and DMA, followed by prior degassing and extrusion through a spinneret into the air. The initial temperature of a spinning solution is mostly over the ambient temperature. As soon as the solution exits extruder and spinneret, the flash evaporation of solvent occurs, and that leads to a solid polymer HF membrane formation. The remaining traces of solvent can be removed by air-drying.

3.1.3 Dry-jet wet spinning

As mentioned earlier, dry-jet wet spinning is the most common technique for the fabrication of HF membrane. Herein, similar to dry spinning, the dissolved polymer solution is extruded from a spinneret into the air, followed by non-solvent coagulation (water). The coagulation bath assists the cooling of polymer spin, subsequent solidification and membrane formation, and removal of the remaining solvent.

3.1.4 Wet spinning

Herein, the dissolved polymer solution is extruded directly into a coagulation bath without providing any air gap. The spinneret is completely submerged into the non-solvent, and the fibers coming out of the coagulation bath are solidified through diffusion interchange between extruded fiber and bath. The general experimental setup for HF membrane fabrication is shown in Fig. 2 [34].

3.1.5 Factors affecting HF spinning process

The membrane characteristics such as wall thickness and pore morphology, including shape and size of pores, are strongly depend on the spinning parameters involved in HF membrane formation. The influencing parameters are the design of spinneret, the flowrate of a dope solution, air gap, fluid viscosity, residence time, extrusion temperature and pressure, take-up speed, coagulation solvent and

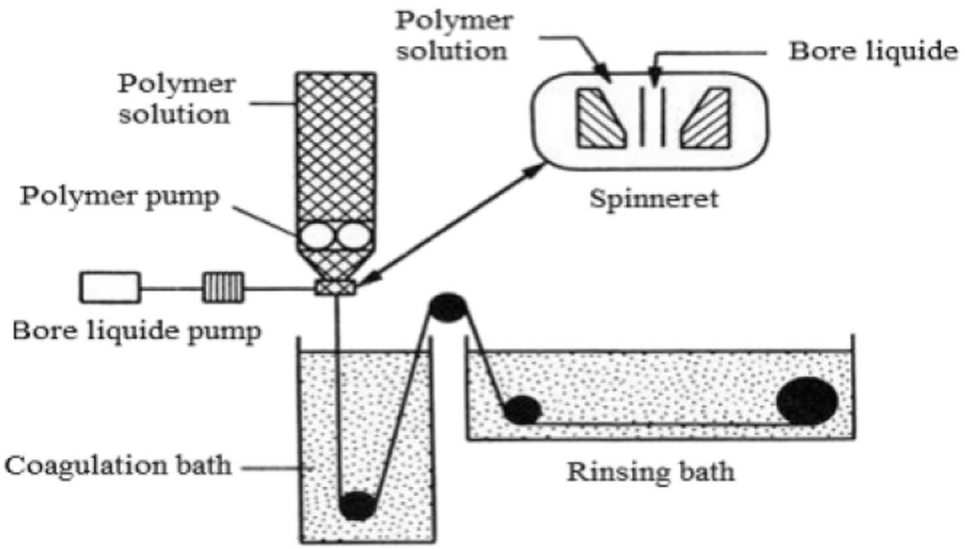

Fig. 2 Schematic representation of HF membrane formation process [29]

bath temperature, total traveling time, and the chemistry of bore fluid. Several studies have reported the influence of these spinning parameters over membrane morphology and properties [35]. Setiawan et al. (2012) reported that, when water is used as a coagulant, the membrane with a dense and smooth surface was formed, while the mixing of water with ethanol or methanol leads to the formation of pores to the outer surface of the membrane [36]. A similar transformation in surface morphology of membrane was observed for IPA as a coagulant. Also, the increment in permeate flux was observed with IPA content up to 60%, and thereafter the flux was reduced imperceptibly [37].

Along with the type of coagulant, the temperature of the coagulation bath also affects the membrane morphology. It was observed that the higher temperature leads to rapid solvent diffusion, which forms the irregular and random pore formation and affects pore volume. In contrast, lower temperatures cause a slower diffusion rate and direct to uniform and regular pore formation [38]. The increase in the flow rate of doping solution enhances outer diameter and wall thickness, further the tensile strength of the HF membrane, while reducing pore size, porosity, and ultimately permeation flux [39, 40]. In addition, the dope extrusion pressure is an important parameter, which must be considered during the HF membrane fabrication process as it also affects the surface morphology and flux of the membrane. The dope extrusion pressure (DEP) is strongly dependent on the flow rate and properties of the dope solution, along with the geometry of the matrix and extruder. The higher extruder pressure may lead to the breakage or the detachment of the outer layer from the inner support of the HF membrane, as the high DEP offers less time for solvent-non-solvent exchange at the interface before the precipitation of precursor in coagulation bath [41]. Shao et al. (2014) observed that, with the increase in DEP during the fabrication of zeolite NaA HF membrane, the length of fingerlike voids has been decreased, which resulted in the retardation of pure water flux (PWF). However, after lowering the DEP from 0.20 to 0.1 MPa, the PWF had been an increase from 1568 to 5142 kg m^{-2} h^{-1} due to an increase in the porosity of the outer layer [41]. Therefore, it is necessary to determine the optimum dope extrusion pressure before the spinning process. The overall relation between DEP and the properties of the membranes can be estimated from the deformation energy, which required overcoming the die parameters such as area of the holes and friction of the inner walls of spinneret [35]. Similarly, each of the spinning parameters affects the entire spinning process and membrane morphology; some of the effects are provided in Table 1 [35].

3.2 Fabrication of TFC hollow fiber membrane

The thin-film composite (TFC) membranes comprise the nano-thin layer and the porous substrate. It can be made by forming a selective barrier over the surface of the porous substrate via different methods such as dip coating, interfacial polymerization (IP), plasma treatment, and chemical reactions [15, 33]. The interfacial polymerization and phase inversion are two main methods used for the fabrication of TFC membranes. The direct phase inversion method is used to fabricate integral skin HF NF membranes, where the substrate and top-skinned layer are made of similar polymeric material. However, the IP is used to prepare TFC membranes with porous support and the skin layer, which are made of different materials, e.g., PSF and aromatic PA [15]. The details related to dip coating and IP is provided below with recent advancement and possible applications.

Table 1 Effects of spinning parameters over HF spinning process [35]

Spinning parameters	Effects
Type of bore fluid	Suppress the collapse of developing HF membrane
Bore fluid temperature	Lower temperature leads to a slower solvent and polymer de-mixing process Higher temperature tends to lower the cooling rate at the lumen of HF
Flowrate of dope solution	Controls the morphology of inner skin
Fluid viscosity	It affects the coagulation kinetics Higher viscosity will promote the chain entanglement of developing HF
Air gap	Plays a vital role in mass transfer for the formation of developing HF More air gap generates defects due to gravity stress and elongation, also increases the residence time of developing HF
Extrusion pressure	It is depending on the properties and flowrate of the dope solution along with the geometry of the extruder Higher pressure may lead to breakage of the outer layer due to less time for solvent-non-solvent exchange at the interface Causes detachment of outer layer from the inner HF support
Take-up speed	It affects the formation of defect-free double-layer HF
Residence time	It is determined from air gap, dope flowrate, and take-up speed
Coagulation solvent	It is used to achieve complete phase inversion (PI) of the outer layer of HF
Coagulation bath temperature	It affects the mass transfer between polymer, solvent, and non-solvent, along with the morphology of HF At higher temperature, the diffusion process of solvent will be in a rapid state Evaluates the crystallinity of developing HF
Total traveling time	Evaluates the retention time of developing HF in the external coagulation bath

3.2.1 Dip coating

The dip-coating method is common in industries for coating fabrics. It is also widely followed by emic researchers, such as for the TFC HF membrane fabrication process. In this method, a nano-metric HF membrane is used as a support. The properties of these composite membranes are inherent in the selectivity and permeability of the membranes. The dip-coating methods involve five different stages such as immersion, start-up, deposition, drainage, and evaporation, respectively. It is generally utilized for the fabrication of self-supportive thin films via a sol-gel method, which is efficient in producing single monolayer thick films [15]. The major disadvantages of dip coating or solution coating are the requirement of suitable solvents by considering its compatibility toward substrate material and thickness of coating film. As a very limited number of solvents are compatible with the polymer substrates, such as for PSF water, aliphatic hydrocarbon solvents and lower alcohols can be used. In addition, in the case of dip coating of HF membranes, to achieve a film with better coating, the substrate must be immersed in the coating solution for several times. This approach may lead to films of higher thickness, which further provides additional mass transfer resistance to the membranes. The thickness of a film depends on the viscosity, concentration of the coating solution, along with volatility of solvent [33]. Therefore, it is necessary to optimize the mentioned characteristics of a coating solution for obtaining better TFC membranes. The general schematic of the dip-coating process for fabrication of TFC HF membrane is shown in Fig. 3.

3.2.2 Interfacial polymerization

The interfacial polymerization (IP) is an in situ and self-growth polymerization thin-film fabrication method utilized for the preparation of high-performance TFC HF membranes. The membranes are first investigated in the 1970s by J. Cadotte [43]. The ultra-thin (20–200 nm) skin layered TFC membranes showed significant advantages over PI-skinned membranes. It is possible to optimize each layer in IP, including nano-thin-film and the porous substrate, for better selectivity, mechanical strength, and permeability of the composite membrane [20, 44].

In this process, two different highly reactive monomers are irreversibly polymerized near the interface of two immiscible solvents to form a thin polymeric film, which is a separation layer in the TFC membrane [20]. The interfacial polymerization process can be described by diffusion-controlled models, wherein the polymerization of monomers in organic and the aqueous phase is supposed to involve the initial stages, which form a dense core layer. The process is later followed by a slow-growth stage of limited monomer diffusion. However, at the interface, a rapid reaction leads to a significantly thinner and dense layer. The selective layer formed via interfacial polymerization is mostly deposited over the lumen side of TFC HF nanofiltration membrane. The concentration of monomers is utilized for governing the

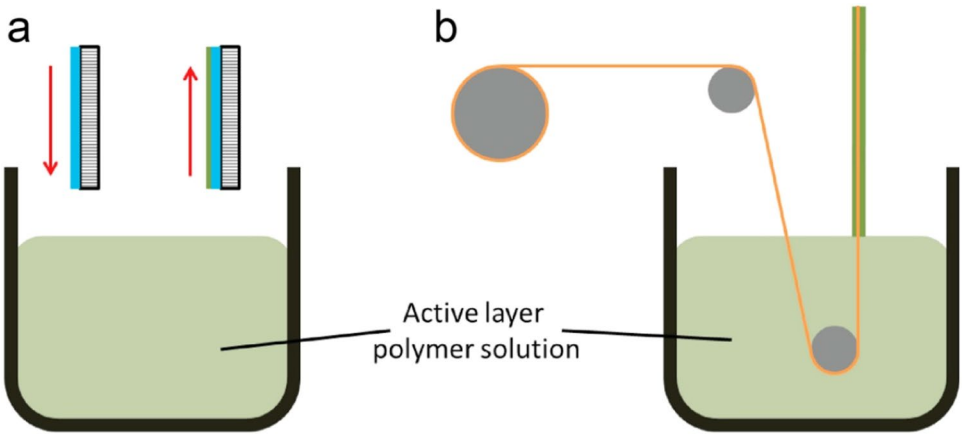

Fig. 3 Schematic representation of dip-coating processes: **a** batch process and **b** continuous process. Reproduced with permission [42]

thickness of the dense core. The factors affecting an IP process include monomers reactivity, partitioning coefficient, growth rate and permeability of polymer film, the reactive concentration of reactants, diffusion rate along with the lag time required during washing of excess monomer solution and at last, the interfacial tension of solvent [20, 45, 46].

The performance of TFC separation layers depends on the structure and morphology, including pore size, roughness, and thickness, along with the hydrophilicity, degree of cross-linking, and functional groups of the membrane. Several monomers such as aliphatic or aromatic diamines and acryl chlorides have been utilized to fabricate TFC HF membranes. The diamines, such as p-phenylenediamine (PPD) and m-phenylenediamine (MPD), and chloride monomers, such as trimesoyl chloride (TMC), 5-isocyanatoisophthaloyl chloride (ICIC), and isophthaloyl chloride (IPC), have mostly been used. However, for TFC HF NF membranes, TMC, PIP, EDA, terephthaloyl chloride (TPC), and hyperbranched poly-ethyleneimine (HPEI) are used extensively [20, 44, 47]. The selection of monomers and their concentration also affect the membrane morphology and ultimately permeability of membranes [48, 49]. In his study, Wu D. (2015) stated that the lower concentration of monomers extends the polymerization process, which results in the formation of loose and thin PA layers with high permeability and low rejection [50].

Along with monomer concentration, the impact of time lag and porous support in the TFC HF membrane is also reported previously. Fathizadeh et al. (2012) explored the effect of interfacial polymerization time lag over the surface properties and separation performance of the PA TFC membrane [51]. It was found that when the porous support has low hydrophilicity and larger pore size with the lowest lag time of IP results in higher water and salt permeability. Also, with an increase in the lag time of IP, the roughness of the TFC membrane decreases and results to lower salt band water permeability. Similarly, Ghosh et al. (2009) reported the effect of various PSF support on the performance of TFC membrane. They concluded that more hydrophobic supports possess higher roughness and permeability due to less PA formed within the pores by interfacial polymerization [52]. However, the studies related to the effect of various IP parameters on the overall performance of TFC HF NF membranes are scant; only some similar studies related to TFC membrane are presented previously. Also, it was found that the developments in the commercialization of TFC HF membranes are lagging behind for several years due to the challenges related to the fabrication of defect-free polyamide (PA) active layer on HF membrane. The hurdle can be overcome by advances in interfacial polymerization methods. Recently, Yang et al. (2021) proposed an unconventional interfacial polymerization methodology for the fabrication of a 1-inch TFC HF membrane module. Also, they have investigated the effect of pressure and flow rates of monomers during the IP process. It was found that a uniform, more robust and defect-free PA selective layer was obtained via circulating m-phenylenediamine (MPD) monomer solution on the lumen side of PES HF substrate at a positive pressure followed by trimesoyl chloride (TMC) solution under the atmospheric pressure. The schematic representation of fabrication of TFC HF membrane module with and without pressure on MDP solution along with respective membrane morphology is shown in Fig. 4. The particular aspects result in the even distribution of MPD monomers on the lumen side of a substrate while retaining its pores for subsequent IP reaction with monomers of TMC. The optimum pressure was found to be 0.1 bar for MPD monomers, whereas the optimal flow rates were observed as 180 mL/min and 17 mL/ min for MPD and TMC monomers, respectively. The obtained membrane had also shown a superior NaCl salt rejection of 98.9% with pure water permeability of 4.49 L m^{-2} $h^{-1}$$bar^{-1}$ and provided comprehensive throughputs for fabricating defect-free TFC HF membrane module for brackish water desalination [53].

Besides dip coating and interfacial polymerization, the TFC membranes were fabricated by specific surface

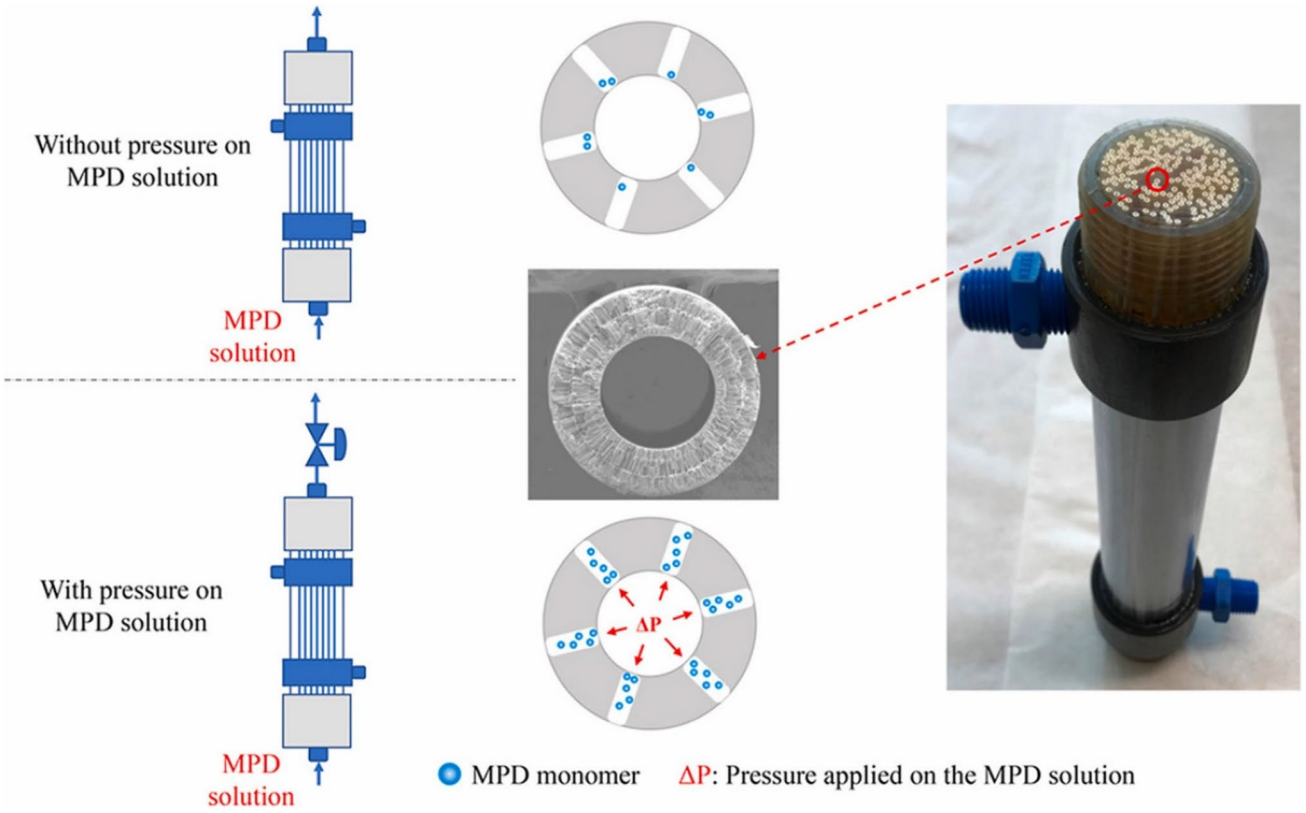

Fig. 4 Fabrication of TFC HF membrane module with and without pressure on MDP solution along with respective membrane morphology. Reproduced with permission [53]

modification techniques such as chemical reactions, plasma treatments, and electromagnetic irradiations [15, 33]. Kim et al. (2011) successfully modified the surface of three commercial nanofiltration membranes, namely, NF90, NF270, and DK, via low-pressure NH_3 plasma treatment. The obtained results had discovered that the surface modification by plasma showed enhancement in the pure water flux (PWF), hydrophilicity, salt rejection, and anti-fouling properties [54]. Although the HF and TFC HF membrane fabrication methods are well developed, the separation performance of these membranes in terms of selectivity and permeation flux must be improved. The surface modification of the TFC membrane with the help of functionalized polymers and nanomaterials could enhance the separation efficiency.

4 Functionalization of TFC hollow fiber NF membrane

The significance of HF NF membranes is well understood for different real-world applications, including seawater desalination and other environmental remediation-related applications. Also, the surface characteristics of TFC membranes have provided great opportunities in the membrane separation processes. However, the surface characteristics of these TFC HF NF membranes can be further improved for enhancing the selectivity, separation efficiency, and flux with the help of its functionalization. Several nanomaterials and polymers are extensively utilized for the functionalization of membranes. These functional materials, with their physicochemical properties, provided additional surface characteristics to the membranes in order to enhance its suitability in environmental remediation applications [47, 48]. The recent developments in the area of nanomaterials such as graphene oxide (GO), Fe_2O_3, CNTs, TiO_2, MOFs, and zeolites had encouraged the world research community to work further for their applications in membrane separation processes via its functionalization [55]. The inclusion of these advanced nanomaterials has assisted in targeting and tailoring the physicochemical properties of membranes. The recent studies have explored the significance of these materials with improved characteristics such as hydrophilicity, higher selectivity, charge density, antimicrobial activity, and superior anti-fouling properties. It is observed that the surface properties influence the permeation, selectivity, and fouling behavior of the membranes. Such parameters may be controlled by tailoring the structure and chemistry

of polymers [56]. The charged and hydrophilic membranes have shown the tendency to improve selectivity and lowering the fouling in membranes [57]. The charged TFC HF nanofiltration membranes are widely utilized for wastewater treatment via electrostatic repulsion and attraction. Similarly, thin-film nanocomposite (TFN) membranes derived via impregnation of nanomaterials, with their hydrophilic nature and flexibility in solutions, have contributed to the removal of water pollutants [55].

4.1 Charge-assisted functionalization of TFC hollow fiber NF membranes

Since the introduction of NF membranes, it has gained a massive interest due to its selectivity toward mono- and multivalent ion separation with low operating pressure, cost, and capital [58]. The surface charges over the NF membranes play a major role in their separation performance [59]. Mostly, the NF membranes are either negatively or neutrally charged in an aqueous environment. However, the polymeric materials are amphoteric in nature, which exhibits the net positive charge in an acidic environment (pH<4) [60, 61]. The specific behavior leads to the misunderstanding over the actual surface charge of membranes made of these polymers [58, 61, 62]. The positively charged HF NF membranes have shown excellent rejection rate and hydrophilicity over multivalent cations such as calcium, magnesium, and lead ions. Alongside, the positively charged membranes are widely utilized for the removal of cationic dyes; heavy metals from textile, pharmaceuticals, paper, and automobile industries [58, 59]. The positively charged TFC HF nanofiltration membranes provided a significant solute rejection rate due to additional electrostatic repulsion and steric hindrance in the water softening process. For these membranes the solute rejection behavior follows a common trend of$MgCl_2$ > $MgSO_4$ > Na_2SO_4 > NaCl. The positively charged membranes were synthesized by grafting, bulk polymerization, IP, and coating. Generally, the polymer macromolecules carrying the amine groups are used for the fabrication of positively charged membranes.

The polymers such as poly(ethylene imine) (PEI), poly(dopamine) (PDA), poly(vinylchloride), and poly(amidoamine) can be used to fabricate these membranes. The charge of these membranes pendent on the dislocation constants and the number of primary and secondary amine groups in the polymers.

4.1.1 Poly-ethylene imine (PEI)

The fabrication of positively charged NF membranes by IP suffers specific technical difficulties due to lower partition coefficient with monomers of high amine groups. However, it was reported that the branched PEI could be successfully impregnated into the TFC NF membrane via an interfacial polymerization process. Gao et al. (2020) developed a new concept for the fabrication of TFC HF NF membrane with an alternative to conventional IP for the removal of heavy metals. The HF membranes were fabricated via blending sulfonated PSF with PES dope solution and PEI as an amine source in the bore fluid. The amine groups were further modified via poly (acrylic acid) (PAA), 1,3,5-benzebetricarbonyl chloride (TMC), and glutaraldehyde (GA). The proposed reaction mechanism between hyperbranched PEI and GA, TMC, and PAA modifiers is shown in Fig. 5. The obtained membranes were precisely design and suitable for heavy metal removal application. The hyperbranched PEI with high molecular weight was used as a higher concentration; it offers excellent interaction with the oppositely charged molecules. It was found that TMC modified membrane is more effective in decreasing the pore size of HF membranes. The Plain_TMC10 membrane has shown the best results by rejecting >90% of both single and mixed cations, with MWCO of 157 Da and pure water flux of 5.14 LMH/bar [63]. Similarly, a skin layer of TFC HF NF membranes was fabricated via interfacial polymerization using branched PEI and TMC. The obtained membranes acquired a positive surface charge with a high PWF of 17 L/m^2 h and an equivalent pore diameter of 1.29 nm [18, 64].

4.1.2 Poly-dopamine (PDA)

The TFC NF membranes fabricated using PDA have shown good structural stability wherein PDA acts interfacial polymerization. Commonly, these membranes were prepared by self-polymerization deposition and coat methods. However, due to the complex nature of PDA, as compared to PEI and PVA it is rarely used for the synthesis of membranes using interfacial polymerization. In one of the studies done by Zhang et al. (2014), the positively charged TFC NF membranes were fabricated by deposition of PDA and grafting of PEI. The results follows the sequence of salt rejection as $MgCl_2$ > $CaCl_2$ > $MgSO_4$ > Na_2SO_4. It was observed that under the optimal conditions, without showing the positive charge, the PDA doped membranes exhibit the flux of 22.8 L/(m^2 h), with a rejection of Na2SO4 as high as 93.5% [65].

4.1.3 Poly amido amine

The positively charges moieties of poly amido amines can easily be doped by grafting its dendrimer over the IP layer. Zhu et al. (2015) provided an effective and facile approach for modification of TFC HF NF membrane via grafting of PAMAM dendrimer. The grafting was done over the interracially polymerized surface of polyethersulfone (PES) for the removal of heavy metals. The grafting process had provided a positive charge surface to the membranes as well as

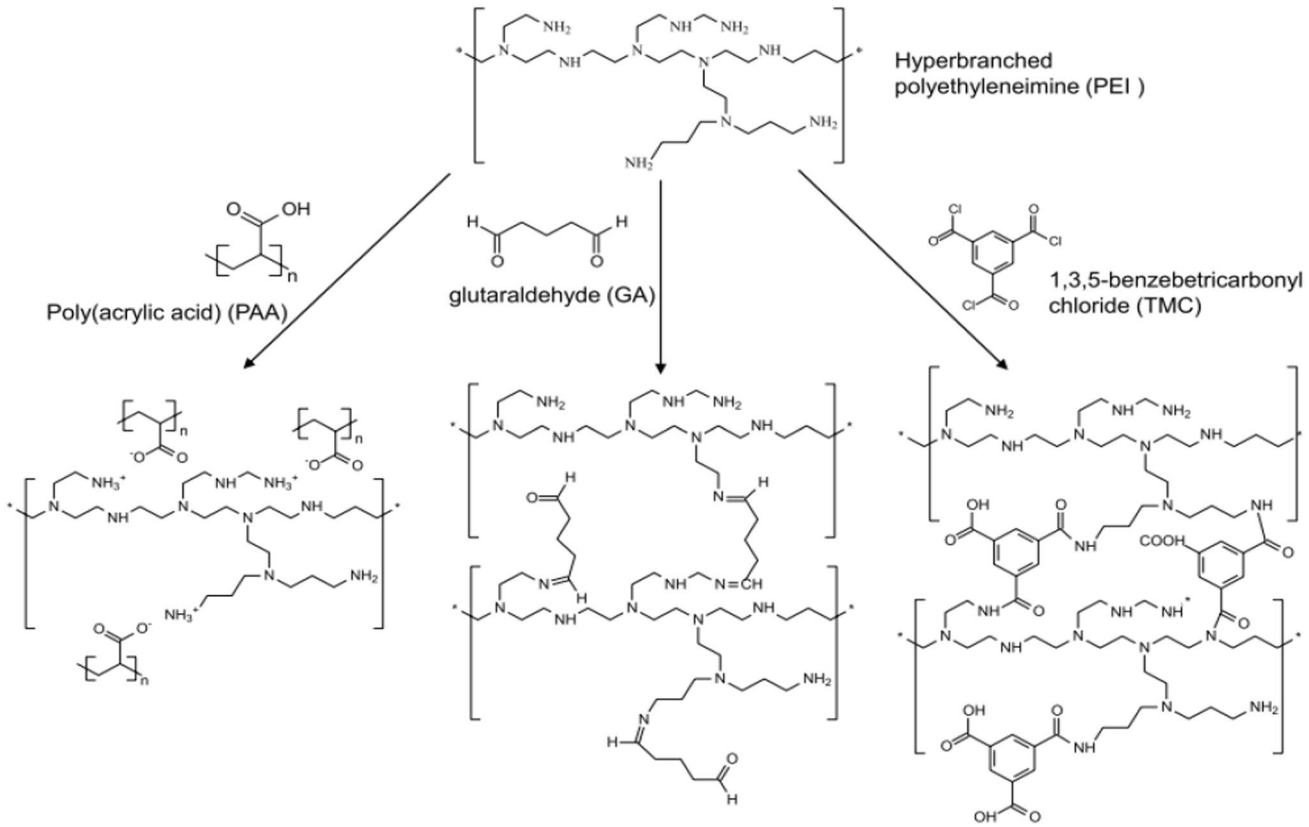

Fig. 5 The proposed reaction mechanism between hyperbranched PEI and GA, TMC, and PAA modifiers. Reproduced with permission [55]

successfully decreased the pore size of the TFC membranes. The resultant membranes had shown good hydrophilicity, ion selectivity, and permeability toward heavy metals. The rejection of >99% was observed for heavy metals such as lead, copper, nickel, arsenic, and zinc [66]. Similarly, in another study done by Li et al. (2017), the carboxylic acid was reacted over the surface of PA TFC membranes using poly (amidoamine) with an activation agent 2-chloro-1-methylpyridinium iodide. The resultant membranes exhibit superior rejection of metal ions such as Ni^{2+}, Cu^{2+}, and Pb^{2+} [67]. The positively charged membranes have shown great potential over the rejection of salts and heavy metals. In particular, PEI has been utilized extensively for environmental remediation applications as compared to other amines. However, the literature related to positively charged TFC HF nanofiltration membranes is very limited; further advanced research is yet to be explored.

4.2 Nanomaterials functionalized TFC hollow fiber NF membranes

TFC membranes are the heart of NF and RO membranes for wastewater treatment and seawater desalination, respectively. Also, several nanomaterials with advanced surface properties, chemical resistance, and their flexibility in solutions provided great opportunities for their real-world application. As stated earlier, recent developments in the area of nanomaterials such as graphene oxide (GO), CNTs, TiO_2, MOFs, and zeolites had encouraged the world research community to work further for their applications in the area of membrane separation processes. Due to the high permeability, low fouling behavior, chemical resistance, and selectivity of nanomaterials have been investigated and applied in various fields [55, 68].

The thin-film nanocomposite (TFN) membrane is termed to be an ideal membrane structure in which the nanomaterials of certain functionalities are embedded within the active layer of membranes. Presently, the synthesis of versatile nanomaterials and their application in HF nanofiltration membranes have gained tremendous attention. Previously the nanomaterials such as graphene oxide, ZnO, TiO_2, metal-organic frameworks, silica are implanted successfully within the active layer of composite membranes [47, 61, 62]. The utilization of these nanomaterials in membranes provides several advantages for TFN membranes, such as high selectivity and permeability, better mechanical, chemical and thermal stability, and antibacterial properties. In addition, the nanomaterials also assist the TFN membranes to

attain specific properties of nanomaterials such as thermal, physiochemical, and optical activities, which offers better separation efficiency, easy operations, and low cost for the membranes [69].

Although these nanomaterials provide certain advantages in separation, there are still few challenges that exist for commercialization, such as nanomaterial selection, leaching in aqueous media, separation performance, and cost analysis. The nanomaterials can improve the permeability of membranes due to micro-porosity and channeling effect; also, the permeability of NF membranes could be enhanced by these two effects of nanomaterials. In the composite membranes, it is anticipated that the nanostructures materials of hydrophilic nature over the outer layer and more hydrophobic substrate on the inner layer will be more favorable for water permeability. Along with the permeability, TFN membranes displayed enhanced anti-fouling properties due to their hydrophilic nature [47, 62].

Recently, Urper et al. (2019) fabricated a TFN HF nanofiltration membrane via IP of polyamide (PA) layer over the shell side of the support. The TiO_2 nanoparticles of varying amounts (0–0.2 wt%) are loaded over the thin film. The resulted membranes have shown 12.6 times higher permeability and higher TOC rejection than the pristine membrane. However, the salt rejection was found to be similar [19]. Similarly, in the other study, the TiO_2 nanoparticles were impregnated over the PSF and CNT blended HF support via dip coating for investigating the anti-fouling behavior of the TFN membrane. The obtained membranes showed 12 folds higher permeation flux with 22% and 5% rejection of MgSO4 and NaCl salts, respectively. However, with anti-fouling behavior, the resulted membranes had successfully rejected 84% and 74% HA and TA, respectively [70].

Liu et al. (2015) developed TFN HF nanofiltration membranes using SAPO-34 nanoparticles on dual-layer PES-PVDF HF substrate. The TFN membrane was fabricated via a solvent-assisted IP process. The resulted membranes had a higher degree of cross-linking and porosity with improved PWF and lower salt permeation. In comparison to NF-90, the obtained membranes have shown higher flux and salt rejection against tris(1,3-dichloro-2-propyl) phosphate, tris(1-chloro-2-propyl) phosphate, and against tris(2-chloroethyl) phosphate with elevated PWP of 20 L/m^2 h bar and tensile strength of 10.3 MPa. In addition, this TFN HF nanofiltration membrane provided enhanced rejection of micropollutants and multivalent electrolytes, presenting potential applications in wastewater treatment and water purification [71].

It is found that the TFN NF membranes are widely explored for desalination and industrial wastewater treatments [72–74]. However, to the best of our knowledge, the research works related to TFN HF NF membranes are scant despite their superior properties, which may be due to the underperformance in salt rejections related studies. It is expected that considering the enhanced surface properties and higher permeability of TFN HF nanofiltration membranes, the research for improvement in the performance will be explored widely in the future. Thus, in the preceding sections, the utilization of TFC NF HF membranes toward various environmental remediation applications has been discussed elaborately to provide a vivid idea about their effectiveness compared to other conventional used methods.

5 TFC hollow fiber membrane for treating textile industry effluent

The textile industry is termed to be one of the key industries all over the world. Presently, it is expected that the rapid increase in the human population will also lead to simultaneous development in the textile industries. Generally, textile industries are considered a significant contributor to environmental and water pollution [24, 46]. It is observed that, in order to produce 1 ton of textile product such as dye, 250–350 m^3 of wastewater is generated [2]. Also, the wastewater produced from the textile industries is mostly having higher BOD and COD. The major contaminants include suspended solids, dyes, oils, electrolytes, minerals, and surfactants [75]. Therefore, it is a must to make sincere efforts to treat and reuse wastewater generated from textiles. Generally, wet processing in textile industries produces major pollutants from raw materials and residual chemical reagents. The color dyes are the key polluting elements generated by textile industries via inefficient dyeing processes. The dyes are mainly characterized as cationic (Rhodamine B, Crystal violet, Brilliant green, and Victoria blue B) and anionic (methyl blue and Congo red) dyes.

Presently, the textile effluent is widely treated by conventional methods such as adsorption, oxidation, coagulation, and biological treatment. However, these methods suffer from sustainably and insufficiency for the treatment of textile wastewater. These treatments aim to destroy or take out the compounds from the wastewater, which affects the recovery and reuse of valuable salts and dyes. The membranes-based separation process had provided various advantages over these conventional techniques. The NF membranes have shown a great potential toward the rejection of water-soluble dyes and salts via size exclusion and electrostatic repulsion phenomenon [23, 76]. The HF NF membranes are extensively utilized for the removal of dyes and other textile effluents due to their compact design, larger surface-to-volume ratio, self-supporting assembly, scalability, and higher permeability. However, the TFC NF membranes showed good rejection of dyes and inorganic salts with low water permeability. Therefore, high transmembrane pressure is required to obtain the higher flux, leading to an increase

in energy requirements. In particular, the TFC HF nanofiltration membranes showed higher selectivity toward dye removal, including the advantages of HF NF membranes [23, 65, 67]. Zheng et al. (2013) developed a TFC HF nanofiltration membrane for decolorization and COD removal of biologically treated water simultaneously. The resultant membrane successfully removed the color and COD by 99% [77].

Similarly, Maurya et al. (2012) fabricated TFC HF NF membranes using PSF UF membrane as substrate and coating the active layer of poly(m-phenylene-trimesamide) via interfacial polymerization. The obtained NF membranes exhibit MWCO of 490–730g/mole and rejection of Rhodamine B and Reactive Black-5 within a range of 60–97% with a flux of 10–35 mL/m^2 h at 25 psi [78]. Also, the recent developments in TFC HF nanofiltration membrane had encouraged the world community for its application in major water polluting industries such as textile. In the present work, details related to the removal of cation and anionic dyes are subsequently provided.

5.1 Removal of anionic dyes

The textile effluent contains toxic azo dyes and inorganic salts, which makes it more challenging industrial effluent. Various methodologies are applied to remove these dyes and salt, where the NF membrane separation process has shown inspiring results by rejecting more than 95% of these dyes. Recently, Ji et al. (2019) developed a TFN HF nanofiltration membrane for the removal of anionic dyes such as Congo red, Acid orange 10, and Direct yellow 24. The PSF/GO loose HF nanofiltration membranes of the dense-loose structure were successfully developed using a one-step non-solvent induced phase separation (NIPS) technique. The membrane filtration was carried out for all three dyes to evaluate the removal efficiency of the obtained membranes. The membrane showed superior results over dye rejection for all the aqueous solutions of dyes with a feed concentration of 100 mg/L. The rejection of Congo red, Direct yellow 24, and Acid orange 10 was obtained at 99.9%, 99.8%, and 78.5%, respectively, with a corresponding flux of 95.4, 98.7, and 101 L/m^2h, whereas the lower salt rejection was at 5% [22]. Ong et al. (2014) fabricated the TFC HF NF membrane using the IP method and systemically evaluated the performance of membranes for rejection of anionic dyes and inorganic salts lab-scale as well as 2 in pitot scale. The separation was carried out at different feed conditions such as temperature, concentration, and pH of the feed solution. The resulted membranes have shown superior performance over rejection of dyes (> 98%) such as Reactive blue 19, Reactive yellow 81, and Reactive black 5. Also, the rejection of inorganic salts was found to be more than 80% and follows the order $MgCl_2$ > NaCl > $MgSO_4$ > Na_2SO_4 [75].

Wang et al. (2018) developed a negatively charged PA/PMIA TFC HF NF membraneby IP method over poly (*m*-phenylene isophthalamide) (PMIA) HF substrate. The obtained membranes have shown superior performance over rejection of salts Na_2SO_4 (98.45%) > $MgSO_4$ (97.98%) > $CaCl_2$ (96.02%) > $MgCl_2$ (95.74%) > NaCl (54.07%) with flux of 104.13 L·m^{-2}·h^{-1} at 0.6-MPa transmembrane pressure. In addition, the performance of resulted membranes was evaluated for three anionic dyes: Reactive yellow 3, Direct Fast Blue B2RL, and Chromotrope FB. The membranes successfully attained the rejection of >97% for all the dyes [2].

Recently, Ji et al. (2021) fabricated PVDF loose NF HF membrane of the multilayered structure via solvent-free green route. Herein, graphene oxide was initially covered over the surface of porous PVDF HF membrane via vacuum filtration, later on for the further modification of HF membrane; the surface was polymerized using polypyrrole (PPy). It was observed that the GO and PPy showed a synergetic effect over the membrane to form a multilayered structure. The obtained membranes showed MWCO of 3580 Da and a pore size of 2.5–4 nm. The performance evaluation of the prepared membrane was done for anionic dye (Congo red, Direct yellow 24, and Acid orange 10), cationic dye (Rhodamine B), and salt rejection. The rejection was observed to be about > 99% for all the dyes except Rhodamine B (94.1) and for salts NaCl and Na_2SO_4, 4 and 12.2%, respectively. The obtained membrane is more favorable for the rejection of dyes [23].

Yu et al.(2012) prepared TFC HF membranes for nanofiltration of anionic dyes using sodium carboxymethyl cellulose (CMCNa) and polypropylene (PP) via the dip-coating method. The outer skin layer of CMCNa was formed by submerging PP microporous HF substrate into the CMCNa solution with the help of a $FeCl_3$ cross-linking agent. It was observed that at neutral pH, the negatively charged membrane showed 99.8% dye rejection for Congo red of 2000 mg/L, with water permeability of 7.01 L/m^2 h bar. However, similar to the previously reported literature, the salt rejection was observed as very low (2%) with 10000-mg/L feed concentration [79].

5.2 Removal of cationic dyes

The generous development of textile industries also leads to various water and environmental pollutants such as dyes. The cationic dye that dissolves into positively charged ions in aqueous media is considered to be most dangerous for human health. Contact with cationic dye may lead to vomiting, jaundice, cyanosis, bladder cancer, and an increase in a heartbeat [80]. Therefore, it is crucial to eliminate these dyes from the effluent of textile industries. Various efforts have been made for the removal of cationic dyes from the effluent

stream using the membrane separation process and adsorption. Recently, Liu et al. (2020) proposed a novel method for the fabrication of TFN NF membranes using carbodiimide-assisted zwitterionic-modified poly(piperazine)amide membranes for removal of both cationic and anionic dyes. The modified membranes had successfully rejected both the cationic and anionic dyes > 90% with good permeate flux [81]. Gao et al. (2017) developed a loose PES HF nanofiltration membrane via a single-step spinning process. The membranes were further modified via sulfonated PSF (SPSF) and more hydrophilic additives such as pore-forming agents PVP and PEG for reducing the average pore size and improving rejection and permeability of the membranes. The PSF/SPSF NF membrane with a smaller pore size was obtained with optimal bore fluid composition of PES:SPSF:PEG 400:NMP:water = 22.5:2.5:18.3:55.2 1.5 (in wt%). The performance evaluated is done for rejection of cationic dyes Alcian blue 8GX (45–65%) and Brilliant blue R (~50%). The rejection of Alcian blue 8GX (45–65%) and Brilliant blue R (~50%) was observed to be >99% with water permeability of 13.39, and 7.28 8 L m^{-2} h^{-1} bar^{-1} [82].

Shao et al. (2013) fabricated novel TFC NF membranes via interfacial polymerization over the lumen side of the PEI HF support membrane. The MWCO of the membranes was achieved as 300 Da by varying the reactive monomers; also, the PWP was obtained as 3.1 L/ m^2 h bar. The membranes were subjected to salt and cationic dye (Aniline blue and Safranin O) removal performance evaluation. It was concluded that, the salt rejection study has shown the rejection trend Na_2SO_4 > $MgSO_4$ > NaCl > $MgCl_2$. Also, the obtained membranes had shown excellent performance over cationic dye rejection with > 90% rejection under the wide range of pH (7–11) [48].

Zheng et al. (2013) developed positively charged TFC HF NF membranes via a dip-coating technique using HF MF membrane support of polypropylene (PP). The coating materials were made of PVA and polyquaternium-10, whereas glutaraldehyde was used as a cross-linker. The cross-linking, hydrophilicity, and membrane morphology were confirmed via ATR-FTIR, contact angle measurement, and FESEM, respectively. A cross-flow permeation test was conducted for estimating the membrane permeation characteristics. However, The dye rejection performance of cationic dye Crystal violet, Brilliant green, and Victoria blue B was evaluated with the help of a submerged filtration test. The obtained membrane has shown excellent dye removal efficiency by rejecting >99% of feed dye solutions of Crystal violet, Brilliant green, and Victoria blue B. In addition, the membranes were tested for salt rejection, and it was observed that a membrane with MWCO 650Da and PWF of 25.7 L/m^2 h had successfully rejected 92.8% of $CaCl_2$ feed solution (500 mg/L) at 3 bar, with the rejection order of $CaCl_2$ > $MgCl_2$ > NaCl > $MgSO_4$ > Na_2SO_4 [83]. Similarly, Wei et al. (2014) fabricated a positively charge TFC HF nanofiltration membrane via IP using reactive monomers such as PEI and TMC. The membranes were exposed to the removal of dye and different salts at different pH conditions. It was found that with an increase in feed concentration of dyes and salts, the rejection rates were decreased gradually. The resulting membranes had successfully rejected the inorganic salt with the sequence of $MgCl_2$ > $MgSO_4$ > Na_2SO_4 > NaCl at pH 7. The cationic dyes chromotrope FB, gold yellow X-GL, and red X-GTL are also subjected to rejection through fabricated TFC HF nanofiltration membranes; the membrane has shown an excellent rejection rate of 98.8, 96.4, and 99.8%, respectively [84].

Based on the provided pieces of literature, it is observed that the TFC HF nanofiltration membranes are much favorable toward both anionic and cationic dye rejection, as compared to salt rejection. Also, the rejection of salt with divalent ions is found to be much higher than the monovalent ions. A further attempt must be made to enhance the performance of the membranes for salt rejection simultaneously. Incorporation of nanoparticles within such membranes could be utilized for enhancing the membrane performance toward textile industry wastewater treatment. Various metallic and bi-metallic nanomaterials have been utilized intensively in various studies where the metallic nanoparticle, due to its electron losing ability, degrades the cationic and anionic dyes when the textile wastewater passes through the membrane. Such nanoparticle-embedded membranes act as fillers within the porous section of the membrane and could lead to membrane choking by creating huge pressure drops. More studies on the improvement of such membrane preparation need to be more carried out for better efficiency results.

6 Application toward environmental remediation purposes

6.1 Heavy metal removal

Nanofiltration has been extensively used for the removal of heavy metals because of its less consumption of energy and moderate operating conditions as compared to reverse osmosis and pervaporation. It is a common practice in nanofiltration to use the interfacial polymerization method for preparing thin-film nanocomposite membranes on porous supports [85]. Li et al. (2021) developed a novel and robust thin-film nanocomposite NF membrane on a macroporous hollow fiber ceramic (HFC) substrate for the removal of heavy metals. In this study, the aqueous solution of graphene oxide integrated with ethylenediamine was deposited on the HFC substrate with the help of vacuum filtration, followed by the fabrication of a thin polyamide film by 1,3,5-trimesoyl chloride and ethylenediamine with subsequent heat treatment.

The developed eGO_3/PA-HFC membrane has significant application potential for heavy metal removal. The rejection rate of both $ZnSO_4$ and $CuSO_4$ was notably higher compared to others metal ions due to the presence of divalent cations and anions. The removal efficiency of the prepared membrane was found to be in the order of $CuSO_4$ (93.33%) > $ZnSO_4$ (92.73%) > $Cu(NO_3)_2$ (90.83%) ≈ $CuCl_2$ (90.97%) > $NiSO_4$ (90.4%) ≈ $ZnCl_2$ (90.18%) > Pb $(NO_3)_2$ (88.35%). It is concluded that the steric bulk and Donnan effect significantly influenced the removal rate of eGO3/PA-HFC membrane for different heavy metal ions. They also reported that the rejection of heavy metal ions was found to increase with an increased concentration of feed solution [26]. In another study, an NF HF membrane consisting of a novel dual-layer polybenzimidazole/polyethersulfone was fabricated for heavy metal removal by Zhu et al. (2014). They observed that the newly prepared membrane has a higher rejection capacity for heavy metal ions. The rejection rate of the membrane to Pb^{2+} and Cd^{2+} was found to be as high as 93% and 95%, respectively. They also reported that when the salt solution is at pH 12, the rejection rate of $Cr_2O_7^{2-}$ can reach up to 98%. The high rejection rate of the membrane may be attributed to the Donnan exclusion, which played a significant role, owing to its amphoteric charge characteristics as well as low adsorption capacity of the membrane for heavy metals on its surface along with increased water adsorption due to its hydrophilic nature [86]. Similarly, Gao et al. (2014) targeted the removal of Pb^{2+} with the utilization of a positively charged NF HF membrane. In this study, a positively charged nanofiltration membrane was molecularly designed by chemical cross-linking modification of hyperbranched polyethyleneimine with P84 porous HF substrates. They observed that the rejection rate of both $Pb(NO_3)_2$ and $MgCl_2$ increases with an increase in the transmembrane pressure. The highest rejection of $Pb(NO_3)_2$ and $MgCl_2$ were found to be 91.05% and 99.06%, respectively, during the application of PEI cross-linked membranes with the smallest critical mean effective pore radius (r_p). The study reveals that Donnan exclusion is the dominant rejection mechanism if the value of r_p is higher than 0.34 nm. In contrast, size exclusion played a significant role in rejection if the value of r_p is lower than 0.34 nm [87]. Moreover, Lan et al. (2021) developed a thin-film nanocomposite HF containing a novel 3-dimensional hollow cup-like macrocyclic compounds having several functionalities and intrinsic size-sieving cavities that were inserted into a polyamide layer through interfacial polymerization on the interior surface polyethersulfone HF substrates for the removal of boron. They reported that the thin-film nanocomposite membrane consisting of sulfocalix (4) arene (SCA4) nanoparticles showed a better result as compared to the blank TFC membrane. The newly prepared thin-film nanocomposite membrane integrated with 0.05 wt% SCA4 showed 37.4%, 32.1%, and 37.5% higher water flux at pH of 10, 8, and 4, respectively. It can be concluded that though both the thin-film composite and thin-film nanocomposite membrane showed almost similar boron rejection of > 97.3% at pH 10 and >87.7% at pH 8, yet the thin-film nanocomposite membrane resulted in much higher water flux due to the presence of 0.05 wt% SCA4 nanoparticles [88]. The feed and the permeate properties of TFC NF membranes for heavy metals are shown in Table 2. It was found that the major principle responsible for the separation of heavy metals by TFC NF membrane is the Donnan exclusion effect. The Donnan exclusion effect is based on the second law of thermodynamics, which deals solely with ionized electrolytes. The criteria resulting in the Donnan membrane equilibrium is the incapability of certain types of ions to diffuse out from one phase to another in a system

Table 2 Comparative analysis of feed and permeate of TFC NF membrane for removal of heavy metal and inorganic salts

Source	Pollutants		Feed (mg/L)	Rejection rate		References
	Heavy metals	Salts		Heavy metals	Salts	
Synthetic wastewater	Cd^{2+}, Pb^{2+}	$MgCl_2$	100	Cd^{2+} = 95% Pb^{2+} = 93%	$MgCl_2$ = 98%	[86]
Simulated tap water	Zn^{2+}, Cu^{2+}, Ni^{2+}, Pb^{2+}	$MgCl_2$	100 300	For 100 mg/L: $Zn^{2+} > Cu^{2+} > Ni^{2+} > Pb^{2+}$ For 300 mg/L: $Cu^{2+} \approx Zn^{2+} \approx Ni^{2+} > Pb^{2+}$ Zn^{2+} = 93.3%, Cu^{2+} = 92.7%, Ni^{2+} = 90.4%, Pb^{2+} = 88.3%	$MgCl_2$ = 94.1%	[26]
Synthetic wastewater	Pb^{2+}	$MgCl_2$	1000	Pb^{2+} = 91%	$MgCl_2$ = 99%	[87]
Synthetic wastewater	Pb^{2+}, Ni^{2+}, Zn^{2+}	$MgSO_4$, NaCl, $MgCl_2$	1000	Pb^{2+}, Ni^{2+}, Zn^{2+} > 95%	$MgSO_4$ = 65% NaCl = 61% $MgCl_2$ = 99%	[21]
Synthetic wastewater	Boron	NaCl	10 1000	For 10 mg/L: boron > 97.3%	For 1000 mg/L: NaCl = 97.1%	[88]

consisting of either polar solvents or water. According to the Donnan principle, non-diffusible fixed charges in one phase when comes in contact with water can be effectively used to regulate the ion distribution in both phases, thereby resulting in an effective separation and product recovery. As such, the high rejection rate of the membrane may be attributed to the Donnan exclusion effect, which played a significant role, owing to its amphoteric charge characteristics as well as low adsorption capacity of the membrane for heavy metals on its surface along with increased water adsorption due to its hydrophilic nature. Moreover, Donnan exclusion is the dominant rejection mechanism if the value of r_p is higher than 0.34 nm, whereas size exclusion played a significant role in rejection if the value of r_p is lower than 0.34 nm [86].

6.2 Organic micropollutant (MP) removal

Nanofiltration is a pressure-driven and more energy-intensive process when compared to other membrane-based systems, viz., ultrafiltration and microfiltration. Despite its higher pressure obligations, the utilization of NF membranes for wastewater treatment containing various micropollutants has gained significant importance in recent times. Different physicochemical properties involved, viz., solubility, size, diffusivity, hydrophobicity charge, solubility, diffusivity, and hydrophobicity, during the nanofiltration process must be understood in order to achieve an effective removal of micropollutants. The most commercialized and successful membrane consists of a typical three-layer structure TFC polyamide membrane. It is made up of a thin composite active layer having a thickness of <100 nm, which is linked to a more open intermediate and a support layer. The most viable reason for the deterioration in rejection performance of the membrane may be attributed to the strong interaction between the membrane polymer and the organic contaminants [89]. Liu et al. (2019) performed molecular docking between several PhACs (viz., carbamazepine, sulfamethoxazole, metoprolol, propranolol, primidone, and trimethoprim) and the polyamide layer. The study investigated the influence of membrane charge characteristics over solute-membrane interaction by the implementation of protonated/deprotonated states. They observed several non-specific and specific interactions between the polyamide layer and propranolol under neutral pH [90].

Moreover, an improvement of the active layer via the addition of nanomaterials and its accumulation over its surface have gained significant interest in enhancing the membrane performance since both adsorption and subsequent diffusion of the micropollutants take place on the active surface layer of the membrane. An improvement in the rejection rate of PhACs, viz., bisphenol A was observed in the case of a chemically modified (graft polymerization and cross-linking method) NF membrane. The chemically modified membrane showed an enhanced rejection rate of bisphenol A (96.9%) compared to the raw NF membrane (74.1%). The reason for the improved bisphenol A removal may be attributed to the steric hindrance of the membrane linked with the polymeric chain since a non-ionic behavior was exhibited by bisphenol A for the selected pH condition of 7.2 [91]. In another study, Paseta et al. (2019) controlled the positioning of nanofillers, viz., metal-organic framework (MOF) bi-layered TFC and observed a significant improvement in the performance of NF membrane. However, it was reported that the addition of different types of MOFs, viz., HKUST-1 (Cu_3(1,3,5-bencenetricarboxylate)$_2$($H2O)_3$) and ZIF93 (Zn(4-methyl-5-imidazolecarboxaldehyde)$_2$), did not show any significant difference in the rejection rate of both naproxen and diclofenac, yet it demonstrated a flux four times higher as compared to the in-house fabricated TFC membrane [92]. An equivalent trend was reported by Dong et al. (2016) for a thin-film nanocomposite NF membrane, fabricated on a support containing in situ embedded nanoparticles of zeolite [74].

Moreover, Liu et al. (2015) observed a simultaneous enhancement of water flux and improved rejection rate against tris(1,3-dichloro-2-propyl) phosphate, tris(1-chloro-2-propyl) phosphate, and tris(2-chloroethyl) phosphate molecules during the utilization of a thin-film nanocomposite HF NF membrane consisting of nanoporous SAPO-34 nanoparticles, as compared to a pristine NF90 membrane [71]. In addition, a thin-film nanocomposite membrane having an optimal quantity of modified silica nanoparticles immersed in a 0–0.3w/v% trimesoyl solution led to an enhanced rejection rate of atrazine (4%) and propazine (7%) as compared to raw NF membrane. The improved performance may be attributed to the smaller pore size (0.35–0.32 nm) of TFN membranes. The strong interaction between the polymer chain and the oleic acid tails of silica nanoparticles eventually led to structural compactness of the membrane, thereby reducing the permeation of solutes through the membrane [93].

6.3 Inorganic salt removal

Due to the unique characteristics of nanofiltration membrane, it has become significantly attractive in selectively removing specific ions or compounds. The most frequently used NF membranes consist of a negative charge, which is unsuited for the removal of hardness in water. As such, the fabrication of a novel NF membrane with a positively charged surface has gained considerable importance for low-pressure water softening [94]. By employing polyethersulfone as the porous support inner layer and Torlon polyamide-imide as the selective outer layer, Setiawan et al. (2014) prepared a dual-layer microporous HF membrane. In this study, a simple polyelectrolyte cross-linking

utilizing polyallylamine was implemented for the fabrication of a positively charged NF-like selective layer. The membrane showed high rejection efficiency of 95.7% for $MgCl_2$ and saltwater permeability of 15.6 L/m^2 h bar during the treatment of synthetic water containing 1000 ppm $MgCl_2$, thereby indicating the positively charged characteristics of the membrane. They further reported that at an operating pressure of 2 bar, the dual-layer NF HF membrane proved to be very significant during its water softening performance, with divalent cation rejection efficiency of 92.3% and 94.2% for Ca^{2+} and Mg^{2+} respectively. However, it was observed that with an increase in the TDS concentration up to 5000 mg/L, the saltwater permeability performance of the membrane along with the rejection rate for Ca^{2+} and Mg^{2+} deteriorates to 12.9 L/m^2/h bar, 81.8%, and 87.8%, owing to the low effective driving force and high ionic strength respectively [95]. In another study, a thin-film nanocomposite was incorporated with nano-TiO_2 nanoparticles, followed by its formation on a HF membrane support. The support material is composed of a mixture of multi-walled carbon nanotubes and polysulfone. The performance of the NF membrane was evaluated under a cross-flow HF nanofiltration system in solutions of NaCl and $MgSO_4$. The study revealed that the membrane surface variables which control the selectivity of membranes toward ionic species were significantly influenced by the addition of nano-TiO_2. The surface charge of the membrane may also affect the salt rejection, partly because of the Donnan exclusion. The result indicated the enhanced retention potential of ionic species due to the presence of nano-TiO_2 in the dual-layer. The rejection rate of thin-film nanocomposite membrane for both NaCl and $MgSO_4$ at a pressure of 3 bar was found to be 2.5% and 25%, respectively. The study concluded that in nano-TiO_2 integrated polyamide layer, the rejection of $MgSO_4$ was found to be less as compared to thin-film nanocomposite membranes, and there was a decreasing trend of $MgSO_4$ rejection with an increasing TiO_2 concentration. However, it was also observed that for a specified TiO_2 concentration performed within a given set of experiments, a slight improvement in $MgSO_4$ rejection rate was obtained with an improvement in membrane permeability [70].

Similarly, Liu et al. (2015) prepared a thin-film nanocomposite HF membrane integrated with nanoporous SAPO-34 nanoparticles, formed on dual-layer (PES-PVDF) HF substrate. The nanoparticle-assisted thin-film nanocomposite membrane was synthesized through co-solvent (dioxane) assisted interfacial polymerization. The TFN (DOX) membrane led to a decreased salt permeability and improved pure water permeability due to its high degree of cross-linking and larger nanoporosity compared to the TFN membrane. The prepared TFN (DOX) membrane showed a significantly higher rejection rate against Na_2SO_4 than NaCl, owing to the negative charge of NF membranes, and it can be attributed to the Donnan effect. It was also observed that with a nanoparticle loading of 0.2wt%, the rejection rate of Na_2SO_4 was found to be higher than 90%. It can be concluded that the novel TFN (DOX) membrane showed high separation efficiency for the inorganic salts along with a higher water flux of 20.1 L/m^2 h bar [71]. The feed and the permeate properties of TFC NF membranes for inorganic salts are shown in Table 2.

Moreover, during the separation of inorganic salts and micropollutants, membrane fouling was observed as a major problem, which retards the separation efficiency of the membrane significantly. The water permeation and membrane-fouling characteristics are significantly affected by the surface properties of the membrane, viz., charge and hydrophilicity. Much research efforts have been dedicated to membrane surface improvement in order to modify the charge properties and hydrophilicity to enhance the fouling resistance of the membrane. Sun et al. (2011) [96] systematically investigated the influence of hyper branched polyethyleneimine (HPEI) molecular weights on the performance efficiency of an HPEI cross-linked single layer polyamide-imide hollow fiber NF membrane. The study reported that HPEI played a substantial role in functionalizing the membranes for the improvement of both the anti-fouling properties as well as the removal efficiency. Still, cross-linking may not be able to cover larger pores of the substrate as compared to interfacial polymerization due to the broader pore size distribution and reduction of the transport channels of the selective layer after cross-linking. Such findings have also been reported in previous studies related to inorganic salts [97, 98]

Consequently, the HPEI cross-linked single layer polyamide-imide membrane may result in flux declination and solute rejection. However, this issue was effectively solved by forming an ultra-thin selective layer on the hollow fiber membrane support via interfacial polymerization of isophthaloyl chloride (IPC) and HPEI [18]. In addition, it is also lethal for membrane separation if the macromolecular proteins block the membrane pores, thereby contaminating the membrane surface. A widely used protein, viz., bovine serum albumin (BSA) can effectively overcome such issues. As such, BSA was chosen as the contaminant, and the permeate flux reduction was selected as the standard of membrane fouling. The anti-fouling capability is considered to be a very important feature in membranes which evaluates not only its application value but also its service life. The inorganic HFC substrates are corrosion resistant, are easy to clean, and have better chemical stability. Li et al. (2021) [26] observed that for $MgCl_2$, the membrane permeability was slightly decreased, owing to the adsorption of BSA on the membrane surface. However, the membrane rejection rate was significantly increased to more than 95% and a stable flux as high as 13.2 $Lm^{-2}h^{-1}$ was obtained after 7 cycles

of pollution recovery tests. An FDR below 5% and an FRR of almost 100% were obtained, thereby indicating that the eGO_3/PA-HFC membrane signifies a very high anti-fouling efficiency. It was concluded that the eGO3/PA thin film on the HFC substrate consists of superior structural rigidity and pressure resistance.

7 Conclusion and future prospective

In this work, the recent advancements in fabrication methods, functionalization, and application of TFC NF HF membrane for treatment of textile industrial effluent and other possible applications toward environmental remediation are critically reviewed. It was found that, during various wastewater treatment applications, membrane fouling needs to be considered a significant constraint due to the presence of organic micropollutants. Since nanofiltration involves nano-range pore size, the fouling is obvious during various environmental remediation applications. Studies have shown that organic fouling severely affects the surface properties of the NF HF membranes, and thus, removal efficiency of heavy metals, organic micropollutants, and other inorganic salts is reduced. Hence, a specific membrane application type of pollutants with the potential to be deposited on the membrane surface and thus affecting membrane efficiency should be identified. Focusing on this direction could lead to an improved membrane surface synthesis with better functionalization and hydrophilicity, along with a detailed study of the feed composition which needs to be treated.

This review discusses the significant role of HF TFC NF membrane as a reliable operation for treating wastewater containing textile dye, heavy metal, organic micropollutants, and inorganic salts. To obtain better-optimized efficiency for a longer period of time, NF alone may not produce sufficient significant results due to various constraints such as membrane blocking and fouling, whereas the hybrid process of NF membrane, which involves the inclusion of other operations with NF membrane application, can incur better results.

- For facilitating better efficiency results toward various mentioned applications in this review discussion, few points need to be focused and carried out toward further research and development studies.
- To maximize the rejection of dye and organic micropollutant through HF NF membranes, priority should be given to the physicochemical interactions between membrane and pollutants. In wastewater, there are various other organic contaminants; attention should also be given to the interactions between different pollutants and their behavior.
- The focus should be made on membrane preparation, controlling surface hydrophilicity and functionalization, which can improve the membrane performance and reduce membrane fouling due to the organic contaminants present in wastewater.
- A combination of advanced oxidation processes coupled with NF HF membrane application could yield better removal efficiency due to the enhanced effect of both degradation and rejection.

Acknowledgments This work is partially supported by a grant (DST/TM/WTI/WIC/ 2K17/84(G)) from the DST (Department of Science and Technology) New Delhi.

Declarations

Competing interests The authors declare no competing interests.

Disclaimer Any opinions, findings, and conclusions expressed in this paper are those of the authors and do not necessarily reflect the views of DST, New Delhi.

References

1. P. Zhong, X. Fu, T.S. Chung, M. Weber, C. Maletzko, Environ. Sci. Technol. **47** (2013). https://doi.org/10.1021/es4013273
2. T. Wang, X. He, Y. Li, J. Li, Chem. Eng. J. **351** (2018). https://doi.org/10.1016/j.cej.2018.06.165
3. L. Reynolds, J. Anim. Sci. **97** (2019). https://doi.org/10.1093/jas/skz258.374
4. Y. Huang, C. Xiao, Q. Huang, H. Liu, J. Zhao, Chem. Eng. J. **403** (2021). https://doi.org/10.1016/j.cej.2020.126295
5. P.P. Das, P. Anweshan, A.S. Mondal, P. Biswas, S. Sarkar, M.K. Purkait, Chemosphere **263** (2021). https://doi.org/10.1016/j.chemosphere.2020.128370
6. P.P. Das, P. Mondal, A. Anweshan, P.B. Sinha, S. Sarkar, M.K. Purkait, Sep. Purif. Technol. (2021). https://doi.org/10.1016/j.seppur.2020.118013
7. A. Deepti, P. Sinha, S. Biswas, U. Sarkar, M.K. Bora, J. Purkait, Water Process Eng **33** (2020). https://doi.org/10.1016/j.jwpe.2019.101108
8. P. Mondal, A. Anweshan, M.K. Purkait, Chemosphere. **259** (2020). https://doi.org/10.1016/j.chemosphere.2020.127509
9. A. Deepti, P. Sinha, S. Biswas, U. Sarkar, M.K. Bora, J. Purkait, Environ. Manag. **259** (2020). https://doi.org/10.1016/j.jenvman.2019.110060
10. N.A. Yaranal, S. Subbiah, K. Mohanty, Environ. Technol. Innov. (2020). https://doi.org/10.1016/j.eti.2020.101253
11. A.D. Sontakke, M.K. Purkait, Ultrason. Sonochem. (2020). https://doi.org/10.1016/j.ultsonch.2020.104976
12. M. Baláž, Acta Biomater. (2014). https://doi.org/10.1016/j.actbio.2014.03.020
13. S.C. Smith, D.F. Rodrigues, Carbon N. Y. (2015). https://doi.org/10.1016/j.carbon.2015.04.043
14. T. Turken, R. Sengur-Tasdemir, E. Ates-Genceli, V.V. Tarabara, I. Koyuncu, J. Water Process Eng **32** (2019). https://doi.org/10.1016/j.jwpe.2019.100938
15. K.C. Khulbe, T. Matsuura, Polymers (Basel) **10** (2018). https://doi.org/10.3390/polym10101051

16. W.J. Lau, G.S. Lai, J. Li, S. Gray, Y. Hu, N. Misdan, P.S. Goh, T. Matsuura, I.W. Azelee, A.F. Ismail, J. Ind. Eng. Chem. **77** (2019). https://doi.org/10.1016/j.jiec.2019.05.010
17. X. Wei, X. Xu, Y. Chen, Q. Zhang, L. Liu, R. Yang, J. Chen, B. Lv, Front. Chem. Sci. Eng. **15** (2021). https://doi.org/10.1007/s11705-020-1943-8
18. S.P. Sun, T.A. Hatton, S.Y. Chan, T.S. Chung, J. Membr. Sci. **401–402** (2012). https://doi.org/10.1016/j.memsci.2012.01.046
19. G.M. Urper-Bayram, B. Sayinli, R. Sengur-Tasdemir, T. Turken, E. Pekgenc, O. Gunes, E. Ates-Genceli, V.V. Tarabara, I. Koyuncu, J. Appl. Polym. Sci. **136** (2019). https://doi.org/10.1002/app.48205
20. G.M. Urper, R. Sengur-Tasdemir, T. Turken, E. Ates Genceli, V.V. Tarabara, I. Koyuncu, Sep. Sci. Technol. **52** (2017). https://doi.org/10.1080/01496395.2017.1321668
21. Y. Zhang, S. Zhang, J. Gao, T.S. Chung, J. Membr. Sci. **515** (2016). https://doi.org/10.1016/j.memsci.2016.05.035
22. D. Ji, C. Xiao, S. An, J. Zhao, J. Hao, K. Chen, Chem. Eng. J. **363** (2019). https://doi.org/10.1016/j.cej.2019.01.111
23. D. Ji, C. Xiao, J. Zhao, K. Chen, F. Zhou, Y. Gao, T. Zhang, H. Ling, Sci. Total Environ. **754** (2021). https://doi.org/10.1016/j.scitotenv.2020.141848
24. G. Li, W. Kujawski, R. Válek, S. Koter, Int. J. Greenh. Gas Control **104** (2021). https://doi.org/10.1016/j.ijggc.2020.103195
25. A.D. Sontakke, M.K. Purkait, Chem. Eng. J. **420** (2021). https://doi.org/10.1016/j.cej.2021.129914
26. P. Li, Y.X. Li, Y.Z. Wu, Z.L. Xu, H.Z. Zhang, P. Gao, S.J. Xu, Environ. Res. **197** (2021). https://doi.org/10.1016/j.envres.2021.111040
27. L. García-Fernández, M. Khayet, M.C. García-Payo, *Membranes used in membrane distillation: preparation and characterization: from pervaporation, vapour permeation and membrane distillation principles and applications* (Elsevier Inc., 2015), pp. 317–359. https://doi.org/10.1016/B978-1-78242-246-4.00011-8
28. S.N. Ashrafizadeh, Z. Khorasani, Chem. Eng. J. **162** (2010). https://doi.org/10.1016/j.cej.2010.05.036
29. C.Y. Feng, K.C. Khulbe, T. Matsuura, A.F. Ismail, Sep. Purif. Technol. **111** (2013). https://doi.org/10.1016/j.seppur.2013.03.017
30. H.A. Tsai, W.H. Chen, C.Y. Kuo, K.R. Lee, J.Y. Lai, Sci. **309** (2008). https://doi.org/10.1016/j.memsci.2007.10.018
31. K.M. Lisboa, J.R.B. de Souza, C.P. Naveira-Cotta, R.M. Cotta, Int. Commun. Heat Mass Transf. **109**, 104373 (2019). https://doi.org/10.1016/j.icheatmasstransfer.2019.104373
32. X. Wei, X. Kong, C. Sun, J. Chen, Chem. Eng. J. **223** (2013). https://doi.org/10.1016/j.cej.2013.03.021
33. P.S. Puri, Gas Sep. Purif **4** (1990). https://doi.org/10.1016/0950-4214(90)80024-F
34. N.E. Vinogradov, G.G. Kagramanov, J. Phys. Conf. Ser. **751** (2016). https://doi.org/10.1088/1742-6596/751/1/012038
35. A.L. Ahmad, T.A. Otitoju, B.S. Ooi, J. Ind. Eng. Chem. **70** (2019). https://doi.org/10.1016/j.jiec.2018.10.005
36. L. Setiawan, L. Shi, W.B. Krantz, R. Wang, J. Membr. Sci. **423–424** (2012). https://doi.org/10.1016/j.memsci.2012.07.030
37. K.J. Lu, J. Zuo, T.S. Chung, J. Membr. Sci. **514** (2016). https://doi.org/10.1016/j.memsci.2016.04.058
38. Y. Raharjo, S. Wafiroh, M. Nayla, V. Yuliana, M.Z. Fahmi, J. Chem. Technol. Metall. **52** (2017). https://www.researchgate.net/publication/321126993. Accessed 29 May 2021
39. R. Sengur, C.F. de Lannoy, T. Turken, M. Wiesner, I. Koyuncu, Desalination **359** (2015). https://doi.org/10.1016/j.desal.2014.12.040
40. K. Praneeth, B.S.K.T. James, S. Sridhar, Chem. Eng. J. **248** (2014). https://doi.org/10.1016/j.cej.2014.02.087
41. J. Shao, Z. Zhan, J. Li, Z. Wang, K. Li, Y. Yan, J. Membr. Sci. **451** (2014). https://doi.org/10.1016/j.memsci.2013.09.049
42. K. Xie, Q. Fu, G.G. Qiao, P.A. Webley, J. Membr. Sci. **572** (2019). https://doi.org/10.1016/j.memsci.2018.10.049
43. J.E. Cadotte, R.J. Petersen, *thin-film composite reverse-osmosis membranes: origin, development, and recent advances:from synthetic membranes (ACS symposium series, 1981)*, pp. 305–325. https://doi.org/10.1021/bk-1981-0153.ch021
44. W.J. Lau, A.F. Ismail, N. Misdan, M.A. Kassim, Desalination. **287** (2012). https://doi.org/10.1016/j.desal.2011.04.004
45. D. Samuel D. Arthur, Wilmington, United States Patent (19), 5,258,203, 1993.
46. D.R. Johnson, K.J. Stutts, D.A. Batzel, V.A. Hallfrisch, J.E. Anschutz, Method of making thin film composite membranes, 1994.
47. W. Xie, G.M. Geise, B.D. Freeman, H.S. Lee, G. Byun, J.E. McGrath, J. Membr. Sci. **403–404** (2012). https://doi.org/10.1016/j.memsci.2012.02.038
48. L. Shao, X.Q. Cheng, Y. Liu, S. Quan, J. Ma, S.Z. Zhao, K.Y. Wang, J. Membr. Sci. **430** (2013). https://doi.org/10.1016/j.memsci.2012.12.005
49. L. Wen, W. Wang, Desalin. Water Treat. **51** (2013). https://doi.org/10.1080/19443994.2013.794909
50. D. Wu, *Thin film composite membranes derived from interfacial polymerization for nanofiltration and pervaporation* (University of Waterloo, 2015)
51. M. Fathizadeh, A. Aroujalian, A. Raisi, Desalination. **284** (2012). https://doi.org/10.1016/j.desal.2011.08.034
52. A.K. Ghosh, E.M.V. Hoek, J. Membr. Sci. **336** (2009). https://doi.org/10.1016/j.memsci.2009.03.024
53. T. Yang, C.F. Wan, J. Zhang, C. Gudipati, T.S. Chung, J. Membr. Sci. **626**, 119187 (2021). https://doi.org/10.1016/j.memsci.2021.119187
54. E.S. Kim, Q. Yu, B. Deng, Appl. Surf. Sci. **257** (2011). https://doi.org/10.1016/j.apsusc.2011.06.059
55. B.S. Ooi, J.Y. Sum, J.J. Beh, W.J. Lau, S.O. Lai, *Membrane separation principles and applications: from material selection to mechanisms and industrial uses* (Elsevier Inc., 2018), pp. 47–83. https://doi.org/10.1016/B978-0-12-812815-2.00002-8
56. R.S. Hebbar, A.M. Isloor, K. Ananda, M.S. Abdullah, A.F. Ismail, New J. Chem. **41** (2017). https://doi.org/10.1039/c7nj00221a
57. R.S. Hebbar, A.M. Isloor, A.F. Ismail, S.J. Shilton, A. Obaid, H.K. Fun, New J. Chem. **39** (2015). https://doi.org/10.1039/c5nj01095k
58. S. Cheng, D.L. Oatley, P.M. Williams, C.J. Wright, Adv. Colloid Interf. Sci. **164** (2011). https://doi.org/10.1016/j.cis.2010.12.010
59. L.F. Fang, M.Y. Zhou, L. Cheng, B.K. Zhu, H. Matsuyama, S. Zhao, J. Membr. Sci. **572** (2019). https://doi.org/10.1016/j.memsci.2018.10.054
60. T. Tsuru, J. Chem. Eng. Japan. **51** (2018). https://doi.org/10.1252/jcej.17we235
61. A.E. Childress, M. Elimelech, J. Membr. Sci. **119** (1996). https://doi.org/10.1016/0376-7388(96)00127-5
62. R. Du, J. Zhao, J. Appl. Polym. Sci. **91** (2003). https://doi.org/10.1002/app.13477
63. J. Gao, K.Y. Wang, T.S. Chung, J. Membr. Sci. **603** (2020). https://doi.org/10.1016/j.memsci.2020.118022
64. W. Fang, L. Shi, R. Wang, J. Membr. Sci. **430** (2013). https://doi.org/10.1016/j.memsci.2012.12.011
65. R. Zhang, Y. Su, X. Zhao, Y. Li, J. Zhao, Z. Jiang, J. Membr. Sci. **470** (2014). https://doi.org/10.1016/j.memsci.2014.07.006
66. W.P. Zhu, J. Gao, S.P. Sun, S. Zhang, T.S. Chung, J. Membr. Sci. **487** (2015). https://doi.org/10.1016/j.memsci.2015.03.033
67. M. Li, Z. Lv, J. Zheng, J. Hu, C. Jiang, M. Ueda, X. Zhang, L. Wang, ACS Sustain. Chem. Eng. **5** (2017). https://doi.org/10.1021/acssuschemeng.6b02119
68. D.L. Zhao, S. Japip, Y. Zhang, M. Weber, C. Maletzko, T.S. Chung, Water Res. **173** (2020). https://doi.org/10.1016/j.watres.2020.115557

69. D.Y. Koseoglu-Imer, I. Koyuncu, Appl. Nanotechnol. Membr. Water Treat. (2018). https://doi.org/10.1201/9781315179070-3
70. G.M. Urper-Bayram, B. Sayinli, N. Bossa, E. Ngaboyamahina, R. Sengur-Tasdemir, E. Ates-Genceli, M. Wiesner, I. Koyuncu, Polym. Bull. **77** (2020). https://doi.org/10.1007/s00289-019-02905-w
71. T.Y. Liu, Z.H. Liu, R.X. Zhang, Y. Wang, B. Van der Bruggen, X.L. Wang, J. Membr. Sci. **488** (2015). https://doi.org/10.1016/j.memsci.2015.04.020
72. Z. Gu, S. Yu, J. Zhu, P. Li, X. Gao, R. Zhang, Desalination. **493** (2020). https://doi.org/10.1016/j.desal.2020.114661
73. Q. Li, Y. Wang, J. Song, Y. Guan, H. Yu, X. Pan, F. Wu, M. Zhang, Appl. Surf. Sci. **324** (2015). https://doi.org/10.1016/j.apsusc.2014.11.031
74. L.X. Dong, X.C. Huang, Z. Wang, Z. Yang, X.M. Wang, C.Y. Tang, Sep. Purif. Technol. **166** (2016). https://doi.org/10.1016/j.seppur.2016.04.043
75. Y.K. Ong, F.Y. Li, S.P. Sun, B.W. Zhao, C.Z. Liang, T.S. Chung, Chem. Eng. Sci. **114** (2014). https://doi.org/10.1016/j.ces.2014.04.007
76. A. Giwa, J. Appl. Sci. Technol. **2** (2012). https://doi.org/10.9734/bjast/2012/1520
77. Y. Zheng, S. Yu, S. Shuai, Q. Zhou, Q. Cheng, M. Liu, C. Gao, Desalination. **314** (2013). https://doi.org/10.1016/j.desal.2013.01.004
78. S.K. Maurya, K. Parashuram, P.S. Singh, P. Ray, A.V.R. Reddy, Desalination. **304** (2012). https://doi.org/10.1016/j.desal.2012.07.045
79. S. Yu, Z. Chen, Q. Cheng, Z. Lü, M. Liu, C. Gao, Sep. Purif. Technol. **88** (2012). https://doi.org/10.1016/j.seppur.2011.12.024
80. V.P. Mahida, M.P. Patel, Arab. J. Chem. **9** (2016). https://doi.org/10.1016/j.arabjc.2014.05.016
81. M. Liu, Q. He, K. Zhang, Z. Guo, Z. Lü, S. Yu, C. Gao, J. Hazard. Mater. **396** (2020). https://doi.org/10.1016/j.jhazmat.2020.122582
82. J. Gao, Z. Thong, K.Y. Wang, T.S. Chung, J. Membr. Sci. **541** (2017). https://doi.org/10.1016/j.memsci.2017.07.016
83. Y. Zheng, G. Yao, Q. Cheng, S. Yu, M. Liu, C. Gao, Desalination. **328** (2013). https://doi.org/10.1016/j.desal.2013.08.009
84. X. Wei, S. Wang, Y. Shi, H. Xiang, J. Chen, Ind. Eng. Chem. Res. **53** (2014). https://doi.org/10.1021/ie5017688
85. M.F. Jimenez-Solomon, P. Gorgojo, M. Munoz-Ibanez, A.G. Livingston, J. Membr. Sci. **448** (2013). https://doi.org/10.1016/j.memsci.2013.06.030
86. W.P. Zhu, S.P. Sun, J. Gao, F.J. Fu, T.S. Chung, J. Membr. Sci. **456** (2014). https://doi.org/10.1016/j.memsci.2014.01.001
87. J. Gao, S.P. Sun, W.P. Zhu, T.S. Chung, J. Membr. Sci. **452** (2014). https://doi.org/10.1016/j.memsci.2013.10.036
88. N. Lan, K.Y. Wang, M. Weber, C. Maletzko, T.S. Chung, J. Membr. Sci. **620** (2021). https://doi.org/10.1016/j.memsci.2020.118887
89. B. Hofs, R. Schurer, D.J.H. Harmsen, C. Ceccarelli, E.F. Beerendonk, E.R. Cornelissen, J. Membr. Sci. **446** (2013). https://doi.org/10.1016/j.memsci.2013.06.007
90. Y.l. Liu, K. Xiao, A.q. Zhang, X.m. Wang, H.w. Yang, X. Huang, Y.F. Xie, J. Membr. Sci. **577** (2019). https://doi.org/10.1016/j.memsci.2019.02.017
91. J.H. Kim, P.K. Park, C.H. Lee, H.H. Kwon, J. Membr. Sci. **321** (2008). https://doi.org/10.1016/j.memsci.2008.04.055
92. L. Paseta, D. Antorán, J. Coronas, C. Téllez, Ind. Eng. Chem. Res. **58** (2019). https://doi.org/10.1021/acs.iecr.8b06017
93. N. Rakhshan, M. Pakizeh, Sep. Purif. Technol. **147** (2015). https://doi.org/10.1016/j.seppur.2015.04.013
94. S.P. Sun, K.Y. Wang, D. Rajarathnam, T.A. Hatton, T.S. Chung, AICHE J. (2010). https://doi.org/10.1002/aic.12083
95. L. Setiawan, L. Shi, R. Wang, Polymer (Guildf) **55** (2014). https://doi.org/10.1016/j.polymer.2013.12.032
96. S.P. Sun, T.A. Hatton, T.S. Chung, Environ. Sci. Technol. **45** (2011). https://doi.org/10.1021/es200345q
97. Z. Yang, P.F. Sun, X. Li, B. Gan, L. Wang, X. Song, H.D. Park, C.Y. Tang, Environ. Sci. Technol. **54** (2020). https://doi.org/10.1021/acs.est.0c05377
98. G. Han, T.S. Chung, M. Weber, C. Maletzko, Environ. Sci. Technol. **52** (2018). https://doi.org/10.1021/acs.est.7b06518